

## ARCUS MISSION DESIGN: STABLE LUNAR-RESONANT HIGH EARTH ORBIT FOR X-RAY ASTRONOMY

Laura Plice,<sup>\*</sup> Andres Dono Perez,<sup>†</sup> Lisa PolICASTRI,<sup>‡</sup> John Carrico<sup>§</sup>, and Mike Loucks<sup>\*\*</sup>

The *Arcus* mission, proposed for NASA's 2016 Astrophysics Medium Explorer (MIDEX) announcement of opportunity, will use X-ray spectroscopy to detect previously unaccounted quantities of normal matter in the Universe. The *Arcus* mission design uses 4:1 lunar resonance to provide a stable orbit for visibility of widely-dispersed targets, in a low background radiation environment, above the Van Allen belts for the minimum two-year science mission. Additional advantages of 4:1 resonance are long term stability without maintenance maneuvers, eclipses under 4.5 hours, perigee radius approximately 12 Re for data download, and streamlined operational cadence with approximately 1 week orbit period.

### INTRODUCTION

The *Arcus* mission, currently in "Step 2" proposal phase for NASA's 2016 Astrophysics Medium Explorer (MIDEX) announcement of opportunity, will be a two-year exploration using X-ray spectroscopy to detect previously unaccounted quantities of the normal matter content of the Universe. *Arcus* will study stars, galaxies, and clusters of galaxies, and will characterize the interactions between these objects. The *Arcus* mission design must provide a stable orbit for visibility of these widely-dispersed targets, as well as provide a low background radiation environment above the Van Allen belts (VAB) for the minimum two-year science mission. Other primary mission design drivers support simplifying the spacecraft and mission operations.

Figure 1 shows the *Arcus* transfer trajectory and lunar-resonant P/4 (1/4 Lunar Orbit Period) orbit for the two-year duration of the nominal science phase. On the left, the trajectory is shown in Earth-Inertial reference frame. On the right, the trajectory is displayed in the Earth-Moon rotating frame with the Earth-Moon line being fixed, and the Moon at the top of the frame. Plotting the trajectory in the Earth-Moon rotating frame provides graphical insight into the P/4 resonance.

---

<sup>\*</sup> Systems Engineer V, Metis Technology Solutions, NASA/Ames Research Center, Mission Design Center, Moffett Field, CA.

<sup>†</sup> Trajectory Analyst, Millennium Engineering and Integration Services NASA Ames Research Center, Moffett Field, CA.

<sup>‡</sup> COO & Principal Aerospace Engineer, Space Exploration Engineering (SEE), lisa@see.com

<sup>§</sup> CTO, Astrogator, Space Exploration Engineering (SEE), astrogatorjohn@see.com

<sup>\*\*</sup> CEO, Astrogator, Space Exploration Engineering (SEE), loucks@see.com

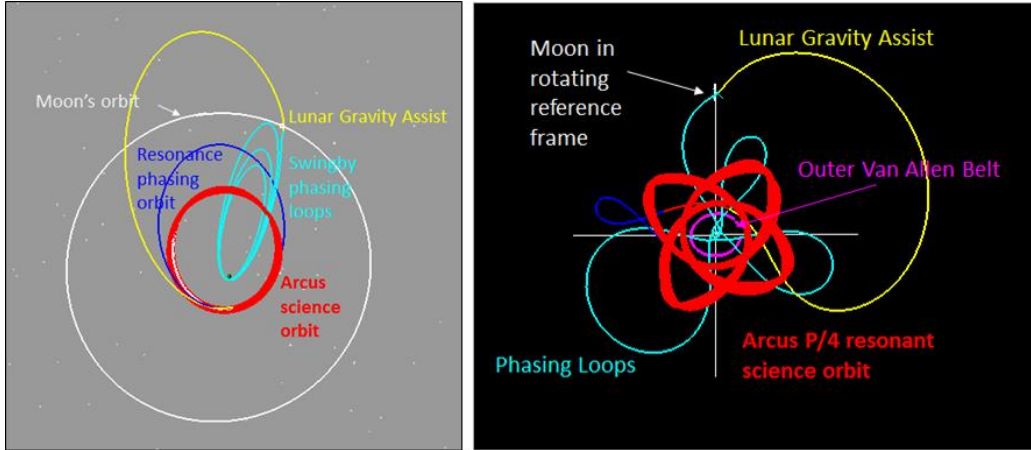


**Figure 1. Arcus phasing loop transfer and 4:1 resonant mission orbit for 2-year science phase**

The trajectory design trades and considerations resulted in a Design Reference Mission (DRM) that uses a stable High Earth Orbit (HEO) for the science phase. A properly oriented science orbit resonant with the Moon’s orbit keeps the apogee away from the Moon, stabilizing the orbit from lunar perturbations while also reducing the propellant needed for orbit maintenance during science operations<sup>1</sup>. The 4:1 lunar resonance pattern (or “P/4”) was chosen for *Arcus*. A lunar gravity assist during the transfer to HEO reduces the delta-v costs, as demonstrated recently by the TESS mission<sup>8,9</sup>. A series of phasing loops are used after launch to target the lunar gravity assist. The collection of mission design drivers, along with the *Arcus* DRM parameters are listed in Table 1.

**Table 1: Arcus Mission Design Drivers and DRM Values**

| Mission Design Drivers  | Limit                 | Arcus DRM Values      |
|---|-----------------------|-----------------------|
| Radiation exposure clear of VAB                                       | Altitude >60,000 km   | Altitude >70,800 km   |
| P/4 resonance, (Phase A trade)  | Orbit period 6.8 days | Orbit period 6.8 days |
| $\Delta v$ budget 373 m/s (3 $\sigma$ low performance)                | 373 m/s               | 294 m/s               |
| Max maneuver size to avoid >1hr burns                                 | 175 m/s               | 130 m/s               |
| Max eclipse duration, thermal management                              | 4.5 hrs               | 3.1 hrs               |
| Minimum Sun angle on thrusters  | > 20 deg (est.)       | 157 deg               |
| Maximum radius distance from Earth                                    | 110 Re                | 93.4 Re               |
| Science orbit equatorial inclination near DSN latitudes (35 – 40 deg) | < 40 deg              | 35 deg                |
| Post-mission Geostationary belt keep-out                              | Altitude >35,986 km   | Altitude >66,438 km   |

## TRAJECTORY AND ORBIT DESIGN

### Arcus Trajectory Overview

Two portions of the *Arcus* trajectory are 3-body solutions in the Earth-Moon system and both parts of the trajectory design derive direct benefit from similar mission experience in phasing loops

for transfer to the Moon and resonant orbits in long term phase with the Moon's motion<sup>1,4,6,7,8,9,10</sup>. The *Arcus* baseline trajectory design approach begins with drivers on the final orbit, then establishes intermediate and initial conditions for the ultimate targets.

A cislunar phasing loop trajectory design is advantageous for absorbing launch dispersions and minimizing trajectory correction delta-v. This technique is used to target the lunar swingby and has been used operationally by several other NASA missions<sup>2,3,4</sup>. Additionally, the use of a lunar gravity assist will add energy to the geocentric orbit, raising perigee to science altitude of nominally 72,000 km, while also effecting an 11 deg plane change.

Figure 2 is an illustration which describes this trajectory as a timeline. The timeline begins at launch on the left and walks through the phasing loops with locations of the lunar swingby phasing maneuvers (SPMs), the lunar encounter, the resonance phasing maneuvers, and correction maneuvers. The timeline from launch until science orbit insertion is approximately 64 days. The 4:1 science orbit will have an average 6.8-day orbit period and eccentricity of about 0.49.

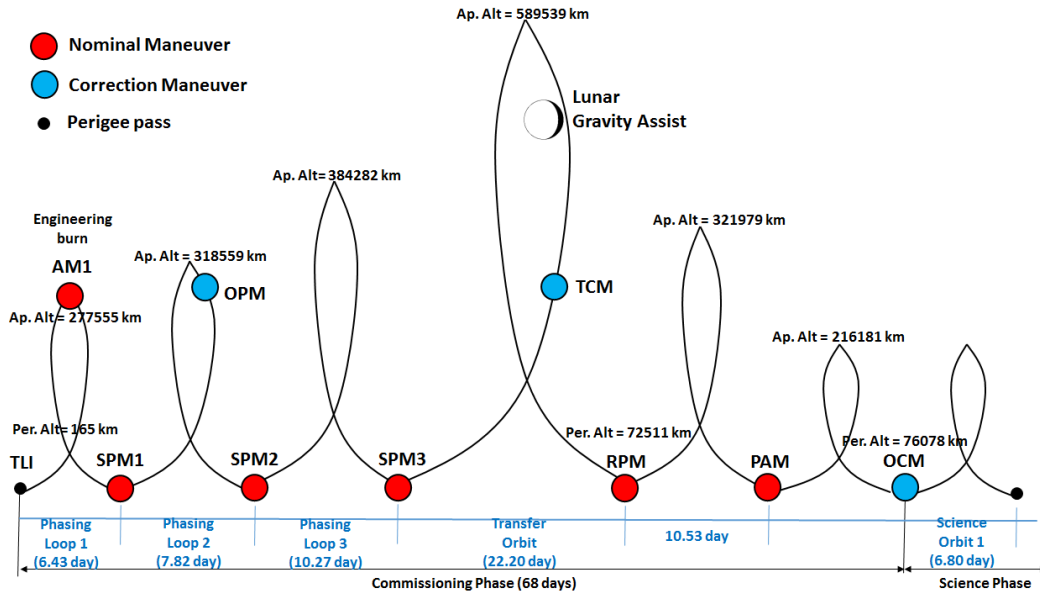
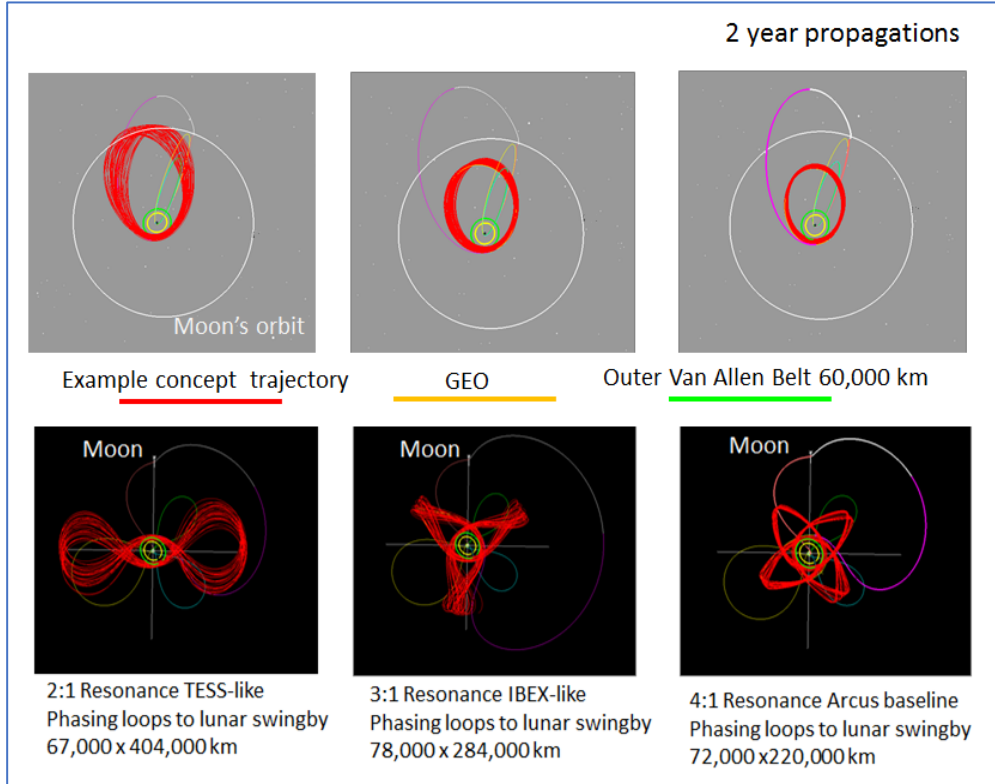


Figure 2: *Arcus* mission profile from launch to the 4:1 resonant science orbit

### *Arcus* P/4 Lunar Resonant Science Orbit

The *Arcus* science orbit benefits from previous work performed in the field of the Earth-Moon resonance environment<sup>1,3,6-11,13</sup>. Figure 3 illustrates early consideration of resonance patterns for *Arcus* and serves as a comparison with widely studied, recent missions, TESS and IBEX.



**Figure 3. Summary of *Arcus* trade studies for science orbit, referencing heritage mission concepts.**

In addition to familiar ratios of P/2, P/3, and P/4, preliminary studies included other relationships. Figure 4 presents an example of numerous available design alternatives, in this case 7/2, (or P/3.5) intermediate between P/4 and P/3.

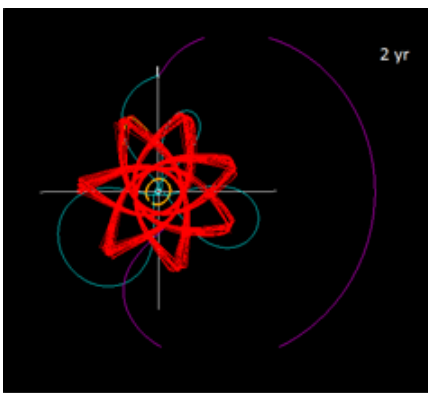


**Figure 4. 7/2 or P/3.5 resonance pattern**

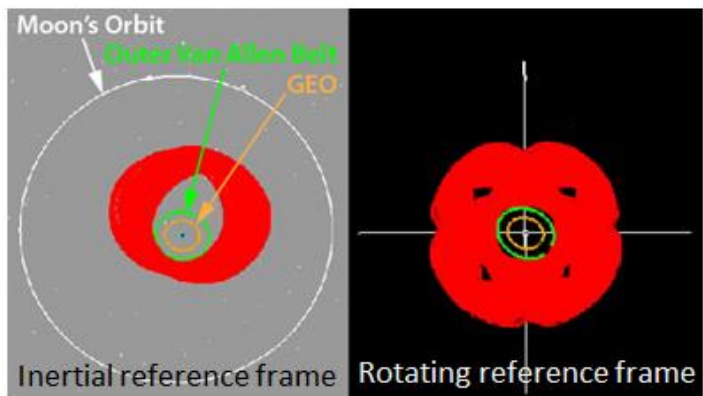


**Figure 5. 100 year resonance in inertial and rotating reference frames**

## Lunar Resonant Orbit Stability and Eclipses

The *Arcus* science orbit—with a lunar resonant P/4 orbit period—benefits from previous work performed in the field of the Earth-Moon resonance environment which investigated a variety of resonance patterns<sup>1,5,6,7,8,9,10,11</sup>. These studies with eccentricities higher than for *Arcus* have shown that although resonant orbits in cislunar space are mathematically unstable, they can be designed so that the divergence from the initial orbit is so slow that they exhibit a practical stability for several decades. In this sense, a major advantage of the *Arcus* science orbit is that the Lunar perturbations on the orbit are predictable, and the closest points to the Moon are maintained at the maximum possible distance for the size of the orbit. This enables prediction of the long-term trends of perigee altitude, the line of nodes, and other parameters including eclipse predictions and communications scheduling. The IBEX mission spent its first two years in a non-resonant cislunar orbit, and the orbit could only be predicted a few years into the future. But after transferring into a similar shaped lunar resonant orbit for its extended mission, the IBEX orbit is stable for more than 20 years under perturbation one thousand times greater than the orbit determination errors. We expect the same or better performance for the *Arcus* science orbit because of its lower radius of apogee radius than IBEX, and so the lunar perturbations will be reduced. Because Monte Carlo simulations were successful for the IBEX and TESS missions, both of which are more affected by Lunar and Solar gravity perturbations than *Arcus* will be, we are confident that the Monte Carlo techniques we've performed, and will perform in preparation for launch, will yield accurate predictions to support mission analysis.

*Arcus* trade studies on the science orbit considered the challenges faced by heritage missions in shadow duration and one of the advantages of *Arcus*' P/4 science orbit is that the maximum hypothetical Earth shadow of 4.5 hours is within tolerance for the spacecraft. With P/4, the *Arcus* mission design enjoys less difficult conditions with respect to perturbations and eclipses than missions with P/2 resonance.

Once established, because the science orbit is resonant with the Moon, it does not require maintenance or deorbit burns. *Arcus*' stable science orbit stays above the geostationary belt (GEO) and the VAB post-mission. Figure 5 illustrates the 100-year propagated science orbit in red, with the Moon's orbit in white, the geostationary (GEO) belt in orange, and the outer VAB in green.

## *Arcus* Transfer Trajectory

The first perigee after the lunar swingby, the Post Lunar Encounter Perigee (PLEP), establishes the proper orientation of the lunar resonant orbit with respect to the Moon at apogee. Lunar swingby parameters target both altitude and orientation relative to the Moon's position at the satellite's perigee pass. The inclination of the mission orbit is not an important science driver and is an effective control for setting up the first perigee.

Figure 6a shows three variations on the same day, with the resulting science orbits similar in altitude and orientation within their orbit planes (but with different inclinations). Case A has a small plane change at the Moon: the orbit plane of the resulting science orbit is near the Earth's equator (center, in green); Case A places the incoming hyperbolic trajectory in the Moon-centered reference frame near the descending node (DN) and has high inclination relative to the Moon's orbit plane (in white), which can create disruptive effects on the *Arcus* orbit's long term stability. Case B places the incoming asymptote for approach near the ascending node (AN) and has a significant plane change during the swingby, creating a science orbit at low relative inclination with respect to the Moon's orbit. The equatorial orbit is moderate and supports DSN contacts, appearing

in Figure 6 as the angle between case B and the interior GEO ring in green. Solutions near the ecliptic plane may have the potential for more frequent eclipses, however with the apogee altitude lower than P/3 or P/2 orbits<sup>3,8</sup>, the maximum shadow duration is manageable. Case C, with the largest inclination change at swingby, is a viable option in terms of orbital mechanics, but results in science orbits with high equatorial inclination, which can decrease DSN contact time, and high relative inclination with respect to the Moon’s plane, where gravitational perturbations appear to disrupt long term stability.

Figure 6b and c illustrate the targeting relationship between inclination and phase angle: some target phase angles are more easily achieved by relaxing the ecliptic inclination constraint. *Arcus* designs use relatively low ecliptic inclination,  $12^\circ \pm 4^\circ$ , and adjust the energy of the post-swingby transfer to set the orientation of the PLEP. Figure 6b is an example from an analysis approach that allows inclination to vary for the purpose of establishing the desired alignment while maintaining approximately the same post-swingby transfer time to the first perigee. Figure 6c illustrates 4 example alignments of the *Arcus* science orbit and identifies the “Phase angle” between the Moon and the first perigee after the Lunar Gravity Assist (LGrA) swingby for solutions in the same orbit plane.

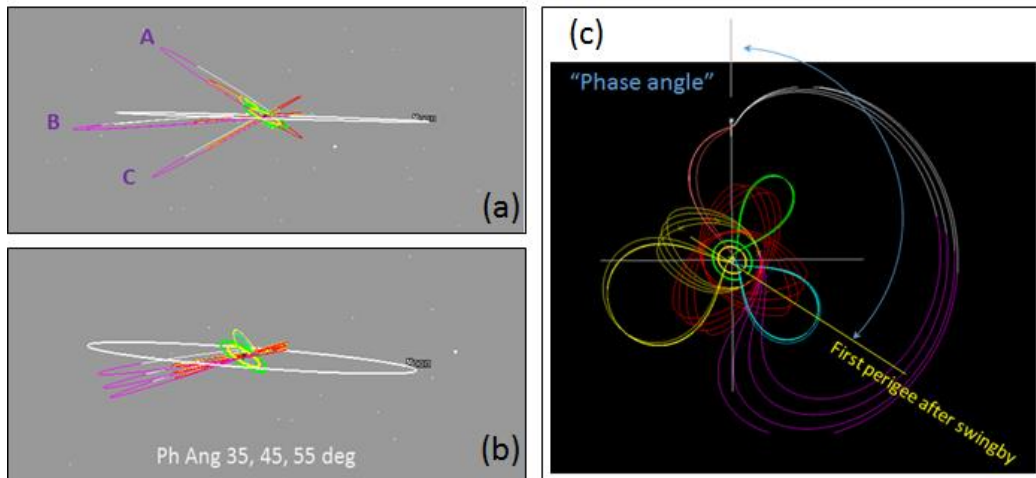


**Figure 6. Associated target parameters of ecliptic inclination, altitude, and phase angle**

Based on evaluation of heritage mission concepts using phasing loops and lunar gravity assist to enter lunar resonant orbit, *Kronos*<sup>6</sup> and *TESS*<sup>8</sup>, *Arcus* compared two main approaches for the post-swingby transfer to the science orbit: 1 maneuver vs 2 maneuvers. A single PAM suits the heritage missions with P/2 resonance and lower delta-v requirements. However, *Arcus* draws advantages from a two-step approach to establishing the science orbit.

*Arcus* post-swingby transfer orbits include two maneuvers, Resonance Phasing Maneuver (RPM) and Period Adjust Maneuver (PAM), for apogee lowering and phasing to  $\frac{1}{4}$  of the Moon’s period, and an Orbit Correction Maneuver (OCM) for correcting dispersions on the large, apogee-lowering burns. Figure 7 compares the two options with the same launch and phasing loops and with the same science orbit result. Additional factors in the number of burn comparison are 12 – 15 extra days in the transfer phase between launch and the arrival in science orbit, and a minor increase in delta-v for greater flexibility of trajectory design. Another benefit of two burns is re-

ducing maximum maneuver size to below 175 m/s, which allows the spacecraft propulsion subsystem to stay within the qualified max burn duration with 3 thrusters instead of needing 4 thrusters to achieve P/4 apogee altitude with a single PAM. The inclusion of an intermediate orbit in the transfer phase has the further advantage of opening up a trade space for targeting a different “lobe” of the resonance pattern at lower delta-v, and accommodating a make-up burn on the next orbit for the missed RPM off-nominal case.

Setting up the alignment of the science orbit in two steps allows substantial flexibility in the *Arcus* trajectory design process. For example, Figure 8 reaches the same resonance orientation for the mission orbit from a wide range of conditions on the intermediate orbit preceding the period adjustment at PAM. Variability in the post-swingby trajectory converges to the same science orbit.

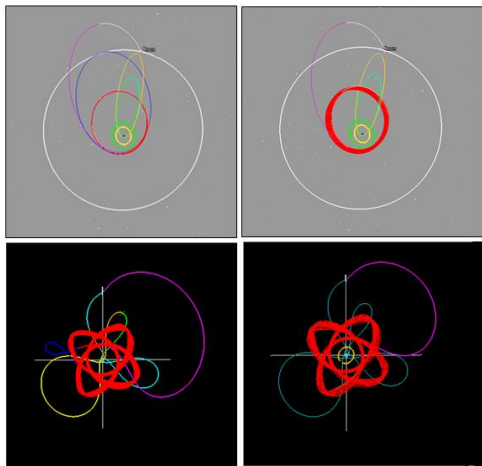


Figure 7. Comparison of Arcus 2-burn (left) and 1-burn (right) transfers to the same P/4 science orbit, in inertial reference frame (top) and rotating reference frame (bottom)

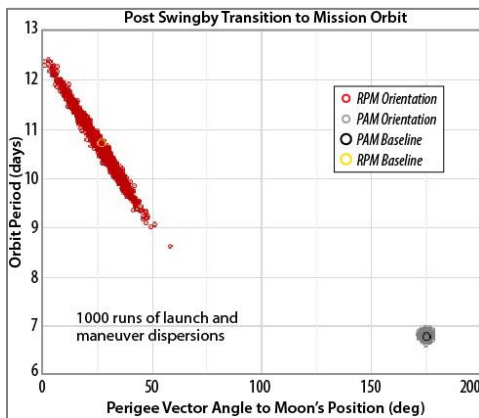


Figure 8. Figure M.14.9-44 Two burns in post-swingby transfer offer great flexibility in trajectory targeting.

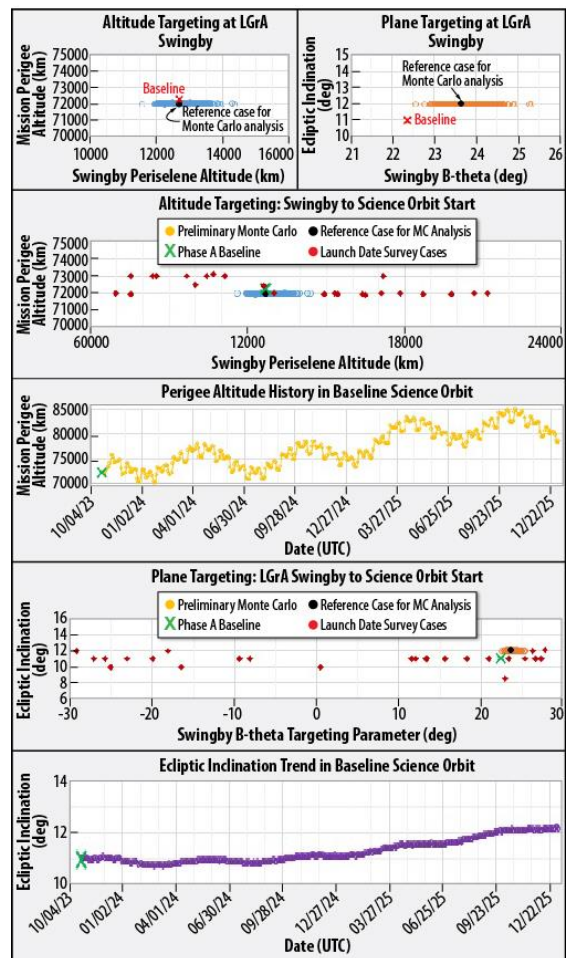


Figure 9. Figure M.14.9-45 *Arcus* trajectory design achieves the desired science orbit with broad flexibility of targeting conditions in the transfer phases.

*Arcus*' two-burn transfer approach easily accommodates dispersions and variations, freeing the design process from stringent targeting requirements to achieve successful mission orbits. Figure 8 illustrates the independence of final orbit parameters from the swingby targeting, including Monte Carlo results of 1000 runs and analytical solutions for launch dates through a complete lunar cycle. In Phase A analyses, P/4 resonant mission orbit designs meeting all requirements vary in perigee altitude from 70,000 to above 80,000 km and in ecliptic inclination from about 8 to 13 deg in trade studies and fluctuate across approx. the same ranges during the science phase.

The flexibility and resilience of the *Arcus* trajectory offer robust recovery options to missed maneuvers, with alternatives and variations available as viable science orbits.

The design method for the *Arcus* trajectory is straightforward use of STK/Astrogator's targeting function using a multivariate predictor-corrector algorithm. Table 2 lists the steps in targeting the *Arcus* P/4 lunar resonant orbit. Phasing loop design to target lunar encounter borrows directly from the *LADEE* trajectory design<sup>4</sup>. McGiffin, Mathews, and Cooley used a similar approach for the *Kronos* P/2 resonant solution<sup>6</sup>.

**Table 2. Outline of steps in targeting *Arcus*' phasing loop transfer to lunar gravity assist and P/4 resonant science orbit**

| Step | Trajectory Phase   | Targeting Event  | Purpose   | Fixed Parameters   | Variables  | Goals / Outcome   |
|------|--------------------|--|---|--|--|---|
| 1    | Launch             | Initial conditions   |   | <ul style="list-style-type: none"> <li>Latitude of launch site</li> <li>Launch azimuth = 90°</li> <li>C3 = -2.75 km<sup>2</sup>/s<sup>2</sup></li> </ul> | Approx. launch epoch   | Post burnout injection state  |
| 2    | Post-launch        | Orbit plane  | Phasing loops intersect Moon's orbit plane      | <ul style="list-style-type: none"> <li>Fixed parameters in Step 1</li> <li>Equatorial inclination of launch site latitude</li> </ul>                     | Coast time   | Angle between the line of apsides of the first phasing loop and the Moon's orbit plane = 0°   |
| 3    | First Phasing Loop | First loop orientation relative to Moon to leverage 3 <sup>rd</sup> body perturbations | Align Phasing loops with Moon's Right Ascension | <ul style="list-style-type: none"> <li>Fixed parameters in Step 2</li> <li>Phasing Loop orbit plane solved in Step 2</li> </ul>                          | <ul style="list-style-type: none"> <li>Launch epoch</li> <li>Coast time</li> </ul>                                   | Angle between the apogee vector of the first phasing loop and the Moon's position at <i>Arcus</i> apogee 1 between 10 and 70°   |
| 4    | Phasing Loops      | Lunar encounter  | Coarse targeting of lunar swingby               | <ul style="list-style-type: none"> <li>Fixed parameters in Step 3</li> <li>Apogee-Moon angle solved in Step 3</li> </ul>                                 | <ul style="list-style-type: none"> <li>Launch epoch</li> <li>Coast time</li> <li>SPM1 Δv</li> <li>SPM2 Δv</li> </ul> | <ul style="list-style-type: none"> <li>Approx. periselene altitude = 10,000 km</li> <li>Approx. B-theta between -20 and 20°, depending on AN vs DN swingby</li> <li>Time of flight from perigee to periselene 3 – 4 days</li> </ul> |



|   |                       |   |  |   |  |   |
|---|-----------------------|---|--|---|--|---|
| 5 | Post-swingby Transfer | Science orbit perigee, inclination, and orientation | Establish science orbit energy and inclination | <ul style="list-style-type: none"> <li>Fixed parameters in Step 4</li> <li>Time of flight solved in Step 4</li> </ul> | <ul style="list-style-type: none"> <li>Launch epoch</li> <li>Coast time</li> <li>SPM1 <math>\Delta v</math></li> <li>SPM2 <math>\Delta v</math></li> </ul> | <ul style="list-style-type: none"> <li>Perigee alt <math>\approx 72,000</math> km</li> <li>Ecliptic inclination <math>\approx 12^\circ</math></li> <li>Per-Earth-Moon phasing angle between perigee vector and Moon's position at PLEP between <math>10</math> and <math>45^\circ</math></li> </ul> |
| 6 | RPM                   | Intermediate orbit period                           | Establish resonance phasing                    | PLEP conditions solved in Step 5  | RPM magnitude  | Per-Earth-Moon phasing angle between next perigee vector and Moon's position at next <i>Arcus</i> perigee = $175^\circ$   |
| 7 | PAM                   | Resonance orbit period                              | Set P/4 orbit period                           | Perigee conditions solved in Step 6   | PAM magnitude  | Science orbit period of 6.76 – 6.84 days  |

### Cislunar Trajectory Maneuvers and the Delta-v Budget

The sequence of maneuvers that comprise the transfer trajectory are shown in Figure 2. Apogee Maneuver 1 (AM1) is an engineering burn, not critical for trajectory execution. Swingby Phasing Maneuvers SPM1 and SPM2 are deterministic trajectory maneuvers based on the baseline insertion orbit, launch day and launch dispersions. After SPM1 execution, SPM2 is retargeted to correct any SPM1 dispersions. SPM3 is an optional maneuver that can be used to correct performance errors in the SPM2 maneuver. An out of plane maneuver (OPM) is budgeted to correct RAAN errors and to allow for wider launch windows. This plane correction is placed off the line of apsides and is used to rotate the RAAN of the pre-swingby phasing loops. The post-swingby transfer trajectory includes two deterministic maneuvers, RPM and PAM, for apogee lowering and phasing to the 4:1 resonant orbit. The final OCM maneuver is statistical, and will be used for precise targeting of the final science orbit parameters.

The process for developing the delta-v budget models a continuum of outcomes with discrete allocations. The temptation to carry a large delta-v budget for flexibility in all circumstances can result in oversizing spacecraft components and even outgrowing the LV. Some allocations map to individual propulsive events; others are calculated estimates with noted distinctions on what they include and exclude.

*Arcus* budgets 373 m/s for baseline trajectory designs throughout the lunar cycle, 30 minute launch windows, launch dispersions, maneuver performance dispersions, finite burn losses, propulsion subsystem calibration, position knowledge error, and orbit maintenance (zero) and deorbit (zero). The two portions of the transfer trajectory, before and after the swingby, each use phasing to the Moon's motion. Each set, first the SPMs (plus OPM) and later the RPM & PAM, include flexible designs for the baseline and corrections to adjust the maneuvers in light of preceding operational conditions. The delta-v budget uses allocations for sets of nominal maneuvers: 50 m/s for phasing loops and 260 m/s for the large, post-swingby maneuvers (Table 3, Items 3 & 7).

A variety of methods and sources inform the *Arcus* delta-v budget in Table 3, including heritage comparisons, parametric studies, corner cases (“hyper-cube” analyses), and Monte Carlo analyses. Allocations target a balance of conservatism for risk mitigation with effectiveness in supporting

spacecraft mass margins and propellant loading and allow groupings of events that are not independent. The columns in Table 3 give the *Arcus* deterministic delta-v budget for the baseline case, estimated or statistical corrections, and budget allocations.

**Table 3: The *Arcus* delta-v budget for deterministic and statistical maneuvers is 373 m/s**

| Mission Event  | Design Reference Mission (m/s) | Worst Analysis Case (m/s) | Delta-V Allocation (m/s) | Item      |
|--|--------------------------------|---------------------------|--------------------------|-----------|
| <b>Part 1 – Phasing Loops</b>                            |                                |                           |                          |           |
| Launch Window Extension                                  |                                | <10                       | 10.0                     | 1         |
| Launch Energy Dispersions                                |                                | 16.0                      | 20.0                     | 2         |
| Launch Plane Dispersions                                 |                                | 13.4                      | 10.0                     |           |
| Swingby Phasing Maneuver 1 (SPM1)                        | 18.0                           |                           |                          | 3         |
| Swingby Phasing Maneuver 2 (SPM2)                        | 19.7                           |                           |                          |           |
| Swingby Phasing Maneuver 3 (SPM3)                        | 0.0                            |                           |                          |           |
| Sum of Phasing Loop Burns                                | 37.7                           | 47.1                      | 50.0                     |           |
| Translunar TCM   |                                | 4.3                       | 10.0                     | 4         |
| A1 Engineering Burn                                      | 2.0                            | 2.0                       | 2.0                      | 5         |
| Total for Phasing Loops                                  | 39.7                           | 92.8                      | 102.0                    | 6         |
| <b>Part 2 – Transfer Orbit</b>                           |                                |                           |                          |           |
| Resonance Phasing Maneuver (RPM)                         | 130.4                          |                           |                          | 7         |
| Period Adjust Maneuver (PAM)                             | 125.3                          |                           |                          |           |
| Sum of Transfer Orbit Burns                              | 255.7                          | 256.0                     | 260.0                    |           |
| Orbit Correction Maneuver (OCM)                          |                                | 8.9                       | 10.0                     | 8         |
| Losses for finite burn, cosine, position knowledge error |                                | 1.0                       | 1.0                      | 9         |
| Total for Transfer Phase                                 | 255.7                          | 265.9                     | 271.0                    | 10        |
| <b>Part 3 – Science Orbit</b>                            |                                |                           |                          |           |
| Orbit Maintenance  | 0.0                            | 0.0                       | 0.0                      | 11        |
| Decommissioning  | 0.0                            | 0.0                       | 0.0                      |           |
| Total for Science Orbit                                  | 0.0                            | 0.0                       | 0.0                      |           |
| <b>Grand Total</b>                                       | <b>295.4</b>                   | <b>358.7</b>              | <b>373.0</b>             | <b>12</b> |

The allocation of 10 m/s for launch window extension in Item 1 reflects LADEE heritage. *Arcus* analyses have found that offsets to the launch time from T-15 minutes to T+15 minutes are affordable within the nominal delta-v allocation. Longer launch windows may be feasible under the 10 m/s allocation.

Figure 10 shows the preliminary analysis of launch energy dispersions and illustrates the resilient nature of the phasing loop approach. Discrete cases for launch energy values in  $\text{km}^2/\text{s}^2$  of -3.25, -3.0, 0.25, -2.5, and -2.25 all converge closely at lunar swingby due to retargeting. Preliminary assessment of trajectory adjustments for launch energy dispersions with a hypercube analysis show corner cases adding as much as 16 m/s to the nominal case, while the estimates for launch plane dispersion alone and 30 m/s for combined launch dispersions (Item 2) used the Monte Carlo approach. Figure 11a, accounts for Items 2 – 5 in Table 3, so the total compares to Item 6.

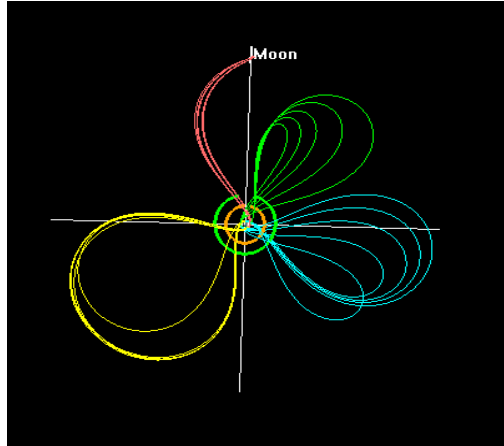


**Figure 10. Launch energy dispersions in phasing loops**

Because launch and maneuver outcomes appear separately, the “Sum of Phasing Loops” subtotal (Item 3) represents nominal cases of SPMs only, with the first column for the baseline case, the middle column for the highest value over a representative lunar cycle, and the right hand column for the budget allocation to cover all identified nominal phasing loop burns. In off-nominal outcomes (still within design dispersions), maneuver magnitudes within coordinated groups trend in opposite directions (Figure 11a and b) so there is no improvement in fidelity by carrying allocations on individual maneuvers.

Performance variations of maneuvers introduce “errors” to the delta-v budget not considered operational contingencies. The phasing loop approach allows corrections of perigee burns to occur at perigee for 1:1 energy cost, so there is no line item for SPM corrections in the delta-v budget. The exception to the perigee corrections is the TCM.

The 10 m/s allocation for translunar TCM in Item 4 reflects the rapid loss of effectiveness of corrections as their placement shifts further and further from perigee. The baseline design leaves perigee 3 free for corrections at 1:1 efficiency. Ideally SPM3 will serve as the correction for SPM2 and achieve final targeting for the lunar swingby. However the TCM allocation covers alternate phasing loop cases where the larger of the SPMs could occur at perigee 3 and takes 20 m/s as a representative value for the larger of two pre-swingby phasing burns. The rationale for the 10 m/s allocation is that a 5% error on a 20 m/s burn would be magnified by about an order of magnitude when applied after 24 hours:  $5\% \text{ of } 20 \text{ m/s} \times 10 = 10 \text{ m/s}$ .

An example case with a large SPM3 would be off-nominal operations where SPM1 was missed. The flexibility of the phasing loop approach to lunar transfer trajectories is such that it may be possible to recover with SPM2 and SPM3. It is also possible to design nominal trajectories which utilize SPM3, however the combination of SPM1 and SPM2 for nominal use offers the advantage of keeping SPM3 small or zero and the likelihood of waiving TCM.

The engineering burn at apogee 1 in Item 5 serves as in flight test of the propulsion subsystem and begins engine calibration. Final calibration requires a complete orbit.

Monte Carlo analyses modeled the maneuver dispersions included in Table 4. Engine calibration is expected to complete after the first phasing loop, however for conservatism the delta-v budget assumes 5% magnitude error throughout. The Monte Carlo method used first introduces errors in each of the nominal maneuvers and propagates the state forward to the next maneuver,

which is then retargeted (based on the errors in the previous maneuver) Therefore, the perturbations are handled, as they would be in actual operations, by recomputing a new solution after each of the maneuvers and adding perturbations to the newly computed maneuver to simulate again the non-perfect maneuver execution.

**Table 4. Dispersion inputs to statistical analyses**

| Maneuver type                          | (3- $\sigma$ ) $\Delta V$ uncertainty           | (3- $\sigma$ ) pointing uncertainty |
|--|---|-------------------------------------|
| Launch TLI                             | 0.5 km <sup>2</sup> /s <sup>2</sup> (C3 energy) | 0.1 deg                             |
| Uncalibrated <i>Arcus</i> prop. system | 5% of nominal solution                          | 5 deg                               |
| Calibrated <i>Arcus</i> prop. system   | 2% of nominal solution                          | 5 deg                               |

The results of 1000 cases are shown in Figure 11 a), b), and c). Figure a) shows of the impact of launch vehicle dispersions on phasing loop delta-v. Differences in the initial C3 cause exchanges between SPM1 and SPM2 as the phasing loop timing adjusts for larger insertion orbits. Initially (with lower insertion C3 values) total phasing loop delta-v decreases with increasing C3, but eventually SPM1 values become negative as this maneuver must take out energy from high insertion loops that must be put back in by SPM2. This can be seen at the point where the delta-v total starts to increase. Plane corrections are related to RAAN errors at insertion, and are a function of higher insertion C3.

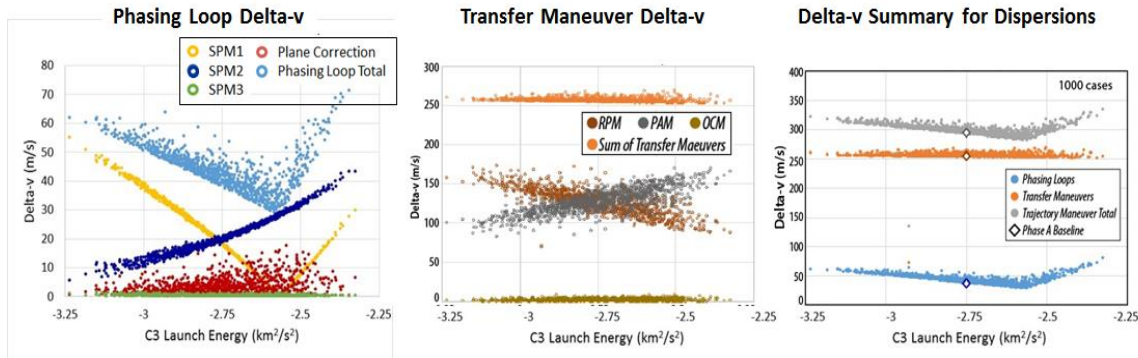


**Figure 11. Statistical calculation of maneuver magnitudes: a) phasing loops, b) post-swingby transfer, c) total**

The results in Figure 11a) show that the *Arcus* phasing loop delta-v needed is well within 92 m/s in Item 6 (launch window extension, controlled by the OPM, is not included in these results so the total allocation reaches 102 m/s). Post-swingby maneuvers in Figure 11 b) are accommodated in the 270 m/s allocated for that portion of the trajectory (Items 7 & 8). While the total delta-v to achieve the science orbit is not a direct function of the launch C3, the RPM and PAM maneuvers play off each other as the timing of the entry to this phase changes with launch C3.

Monte Carlo analyses offer robustness in evaluating potential variations and mitigate “worst-upon-worst” case over-conservatism. OCM sizing in Item 8 is an example where insight into delta-v consumption for individual events is available with the “hypercube” method. Table 5 presents analysis results where the *Arcus* design reference case has conservative maneuver performance

variations of 5% in the RPM and also 5% variation in the PAM. The analysis approach for estimating this allocation applies the 5% overburn or underburn dispersion to the RPM and retargets the PAM, then applies 5% overburn or underburn to the new PAM, then corrects one orbit later with the OCM. The final column compares the retargeted sum of delta-v against the nominal allocation for RPM and PAM, to enable the analysis to inform the allocation for the OCM line item. For the post-swingby maneuvers, Resonance Phasing Maneuver (RPM) and Period Adjust Maneuver (PAM), conservative maneuver errors of  $\pm 5\%$  drove the final Science OCM dv allocation of 10 m/s. Monte Carlo results in Figure 11b) confirm that 10 m/s is a comfortable allocation for the science orbit correction.

**Table 5. Analysis corner cases for Orbit Correction Maneuver (OCM)**

| Error Case      | Nominal RPM dv (m/s) | 5% RPM Error (m/s) | Retargeted PAM dv (m/s) | 5% PAM Error (m/s) | OCM dv* (m/s) | Total Post-swingby dv (m/s) | Vs. 260 m/s Nominal Allocation (m/s) |
|-----------------|----------------------|--------------------|-------------------------|--------------------|---------------|-----------------------------|--------------------------------------|
| <b>Nominal</b>  | 130.4                | 0                  | 125.3                   | 0                  | 0             | 255.7                       | -4.3                                 |
| <b>+5%, +5%</b> | 130.4                | 6.52               | 119.4                   | 5.97               | -6.58         | 268.9                       | 8.9                                  |
| <b>+5%, -5%</b> | 130.4                | 6.52               | 119.4                   | -5.97              | 6.11          | 256.5                       | -3.5                                 |
| <b>-5%, +5%</b> | 130.4                | -6.52              | 131.0                   | 6.55               | -6.27         | 267.1                       | 7.1                                  |
| <b>-5%, -5%</b> | 130.4                | -6.52              | 131.0                   | -6.55              | 7.52          | 256.4                       | -3.6                                 |

\* Positive delta-v values for nominal anti-velocity direction.

The *Arcus* trajectory design assumes accurate knowledge of the spacecraft position at maneuver execution; results from heritage missions indicate that position knowledge will place maneuver execution within one minute of orbit perigee, which is within even the shortest nominal maneuver duration. Preliminary analysis of cosine and finite burn losses are well under 1.0 m/s in Item 9.

Item 10 subtotals are supported by Monte Carlo results in Figure 11c) and the worst case end-to-end delta-v (358.7 m/sec) allows contingency against the total 373 m/s budget.

### Launch Analyses

The launch vehicle has not yet been selected for *Arcus*, however the mission is currently planned to launch from either Wallops Flight Facility (WFF) or Kennedy Space Center (KSC). Launch opportunities occur on most days of the lunar cycle, with launch windows of at least 30 minutes. The *Arcus* launch parameters are summarized in Table 6.

**Table 6: *Arcus* Baseline Launch Parameters**

|                                      |                                       |
|--------------------------------------|---------------------------------------|
| <b>Launch Date</b>                   | September 7, 2023                     |
| <b>Launch Site</b>                   | WFF or KSC                            |
| <b>Insertion C3</b>                  | -2.75 km <sup>2</sup> /s <sup>2</sup> |
| <b>Injection Argument of Perigee</b> | 300 degrees (after 48-minute coast)   |
| <b>Launch Opportunities</b>          | 24-26 days/month                      |
| <b>Launch Window</b>                 | 30 minutes                            |

Preliminary analysis addressed a sample lunar cycle in the calendar month of September, 2023 and found viable solutions on all but 3 launch days. Because of the regular pattern of the Moon’s motion, it is valid to assume that all lunar months will have approximately similar opportunities. Figure 12 shows successful launch dates in the preliminary survey from 7 Sept to 5 Oct 2023. Gaps show missing days and overlaps due to variations in the alignment of the phasing loops to the Moon’s motion.

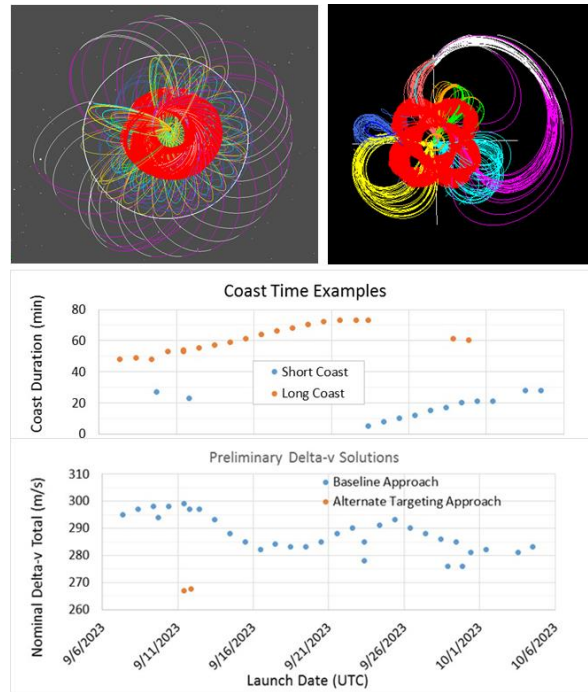


**Figure 12. Preliminary analysis of launches in a lunar month**

For Phase A, most launch dates in the analysis have a single trajectory case. Follow-on trade studies will compare launch dates across ascent profiles and design options, such as Fixed AOP, Short coast, and Long coast. Rationale for investigating multiple options per launch day are mitigation of unfavorable eclipse geometry, flexibility in launch time of day, and simple robustness in the metric of number of launch opportunities.

The coast times before the injection maneuver by the LV upper stage vary as the orbit geometry trends across the lunar cycle. Figure 12 shows coast times and trends in deterministic delta-v for the preliminary set of launch dates.

Eclipses are a major design driver on launch dates. Most solutions with strong similarities to the baseline case have the natural limit on the duration of Earth shadow in the science orbit of 4.5 hrs. (With variations in the apogee altitude, it is possible to exceed the 4.5 hr limit slightly.) Short coast and long coast opportunities on the same day don’t typically create significantly different trajectory solutions, so the resulting science orbits tend to have similar eclipse characteristics since they transit largely the same areas of inertial space in the same timeframe as one another.

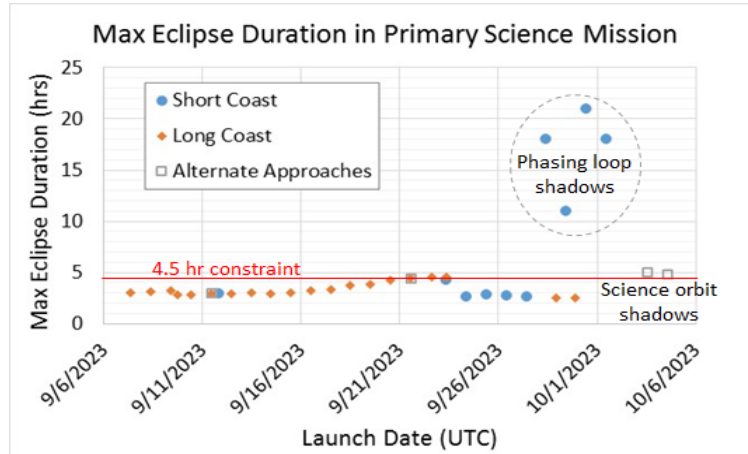


Figure 13. Preliminary Eclipse Analysis for Launches in One Lunar Cycle

Other than changing the target inclination, some fine tuning is possible for slight decreases in the max eclipse duration, for example to meet the max duration requirement, but the differences are generally less than 0.5 hr or shifting the occurrence to the next orbit. Parameters that can vary the design include target science perigee altitude, inclination, and slight modifications of the orientation of the orbit’s line of apsides. The design limit of 4.5 hour eclipse does occur for launches during a portion of the lunar cycle.

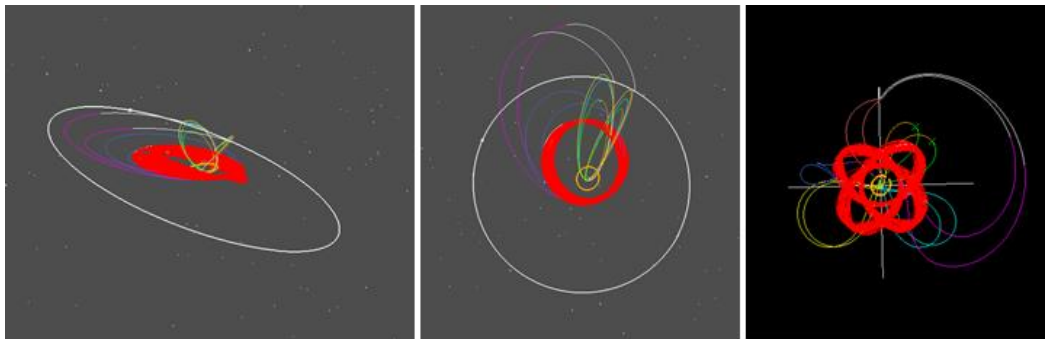


Figure 14. Example Short- and Long-coast solutions on 28 Sept 2023

Eclipses during phasing loops can be much longer than the max limit due to the high eccentricity and resulting slow velocity. Figure 13 shows examples on Sept 28 – 30 of eclipses far exceeding the spacecraft tolerance. Because alternate options for the ascent result in very different phasing loops, it is possible in some cases to avoid eliminating launch days by using a different launch profile (e.g. long coast vs short coast). Figure 14 illustrates an example same-day alternatives.

### GROUND SEGMENT DESIGN

The *Arcus* ground segment includes NASA’s Deep Space Network (DSN), NASA’s Tracking Data Relay Space System (TDRSS), NASA Ames’ Multi-Mission Operations Center (MMOC), and a Science Operations Center (SOC). SN will be used throughout the mission for tracking, telemetry, and commanding (TT&C), from post-launch through all of the maneuver operations, and routinely throughout the science mission operations. TDRSS will only be used for monitoring

maneuvers if the DSN is not in-view during the critical maneuvers. The MMOC functions include spacecraft command and control, flight dynamics, activity planning and scheduling, verification, and engineering tools. The SOC is located at Smithsonian Astrophysical Observatory (SAO), with science data archived at NASA’s High Energy Astrophysics Science Archive Research Center (HEASARC).

### Ground Network & Tracking Design

The ground station network design baselined throughout the mission is NASA’s DSN. The DSN ground network includes the 34-meter antennas at Goldstone, Canberra, and Madrid. The DSN will perform two-way coherent Doppler and Sequential Range tracking with *Arcus*.

The current *Arcus* tracking plan is for three DSN tracking contacts per 6.8-day orbit for orbit determination. These tracking contacts are approximately located as follows: one ascending out of perigee, one at/near apogee, and one on the descending side from apogee towards perigee. Additionally, a fourth DSN contact (not needed for orbit determination) will be planned for about five hours during each perigee for science data downloads. Table 7 breaks-down the ground station scheduling design by mission phase:

**Table 7: *Arcus* Design for Ground Station Supports by Mission Phase**

| Phase                            | Duration | Ground Contact Schedule   | Key Events   | Additional Event Coverage       |
|----------------------------------|----------|---|--|---------------------------------|
| S/C Activation & Checkout        | 2 days   | TT&C (6 hr) each day  | Initial Acquisition<br>Spacecraft Acquisition  | 2 hr (SN), 12 hr (DSN)<br>6 hr  |
| Phasing Loops                    | 26 days  | Pre-SPM2:<br>TT&C (1 hr) each day<br>Post SPM2:<br>TT&C (1 hr) each day     | AM1, OPM, TCM<br>SPM1, SPM2, SPM3  | 7 hr each<br>8 hr each (SN/DSN) |
| Orbit Insertion                  | 36 days  | TT&C (1 hr) each day  | RPM, PAM, OCM  | 7 hr each                       |
| Instrument Activation & Checkout | 20 days  | One SDDL (7 hr) per orbit<br>Three TT&C (1 hr each) evenly spaced per orbit | Power On   | 7 hr                            |
|                                  |          |   | Functional Test  | 7 hr                            |
|                                  |          |   | Instrument Checkout (4 days)   | 7 hr per day                    |
|                                  |          |   | Focal Plane Testing  | No additional                   |
| Door Deployments                 |          |   | Door Deployments   | 7 hr                            |
|                                  |          |   |  |                                 |
| Instrument Commissioning         | 34 days  | One SDDL (7 hr) per orbit<br>Three TT&C (1 hr each) evenly spaced per orbit | Optical Axis Determination<br>Dispersion Determinations<br>Effective Area Calibration<br>Light Leak/Vignetting | No additional                   |
| Science                          | 730 days | One SDDL (7 hr) per orbit<br>Three TT&C (1 hr each) evenly spaced per orbit | Routine ops  | No additional                   |
| Decommissioning                  | 1 day    |   | Passivation  | 7 hr                            |

SDDL: Science Data Downlink. TT&C: Telemetry, Tracking, & Commanding. DSN: Deep Space Network. SN: Space Network. All contacts with DSN unless otherwise noted.

The figure below is a plot of *Arcus*’s altitude over time in science phase, over about 9 orbits (green). With exception of the first orbit, a simulated routine science phase tracking plan is shown (blue segments) with three tracking segments per orbit.



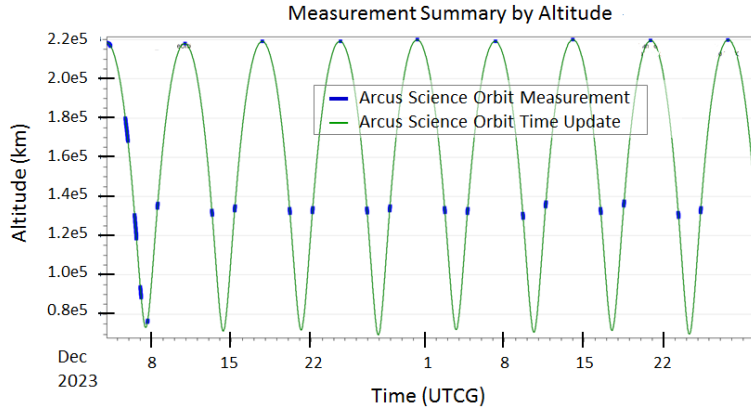


**Figure 15: Arcus Tracking Schedule Design in Science Phase by Altitude**

### Mission Design & Operational Tools

For *Arcus* mission design and analysis our team used Analytical Graphics Inc.’s (AGI’s) Systems Tool Kit (STK) and Orbit Determination Tool Kit (ODTK) extensively. We used the STK/Astrogator module<sup>12</sup> for the entire end-to-end trajectory design because it has been used extensively for analysis and operations in cislunar, lunar resonant, deep space, and gravity assist missions<sup>3,13,14,15,16</sup>. We used ODTK similarly because it has been used it for cislunar analysis and operations, including operations for IBEX’s lunar resonant orbit<sup>13</sup>. During this mission design and analysis phase for *Arcus* we used ODTK to simulate tracking data and perform for orbit determination error analysis. We also used STK with ODTK to create tracking schedules, tables and graphs, and for visualizing ODTK results.

For the repetitive parametric and Monte Carlo simulations, we automated STK using its COM Application Interface (API). We used the Python language using Jupyter Notebooks<sup>17</sup> to loop through launch period cases, setting inputs in STK/Astrogator, commanding STK/Astrogator to propagate and re-target the trajectories, and then to pull data out into tables that we could analyze.

*Arcus* mission operations will include the Flight Dynamics System (FDS), used on the NASA missions IBEX, LADEE<sup>18</sup>, CYGNSS, and TESS, as well as for the commercial SkySat constellation<sup>19</sup>. The FDS is provided by Applied Defense Solutions (ADS) and will be used by the flight dynamics team for trajectory and maneuver planning, orbit determination, and product generation. AGI’s STK and ODTK packages are components of this FDS. The FDS streamlines operations by pulling data from databases, setting parameters in STK and ODTK, running jobs, creating data products, and delivering the products. The FDS is designed to automatically run jobs according to a schedule, but also enables the orbit analyst to run things manually, and if needed, to interact with STK and ODTK directly.

### ORBIT DETERMINATION

*Arcus* primarily carries prediction requirements. Predictions are only needed to support the operational activities of maneuver planning and sending acquisition and scheduling products to the Deep Space Network (DSN). There are no accuracy requirements for science activity planning or for science data processing. Definitive orbit knowledge is only necessary for maneuver reconstruction and general prediction trending. The orbit determination approach reflects the goals to simplify mission operations.

The predicted orbit uncertainties for two orbits are shown in the following graphs. The last tracking time is at apogee around January 15, 2024, however the filter process is run past the last tracking time by two orbits. Meaning, the uncertainty at the time of the last tracking measurement is then propagated for two orbits. In the predicted position uncertainty, the in-track component uncertainty spikes largest near two perigees in the future (January 24, 2024). This is normal to see for elliptical orbits with predictions through perigee. We also graph predicted uncertainty in semi-major axis and in true argument of latitude. The uncertainty 2 weeks out (2 orbits) is still well within the half-power beam width of the DSN 34-m antennas for S-Band transmit and receive.

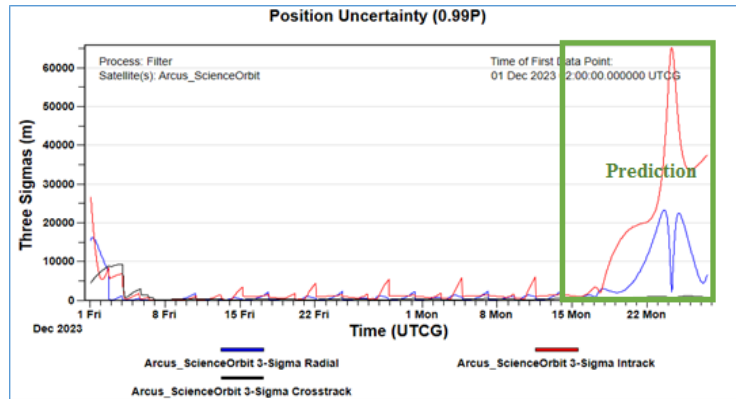


**Figure 16. Filtered 3-Sigma Position Uncertainty, Definitive Span Followed by Predicted Span**

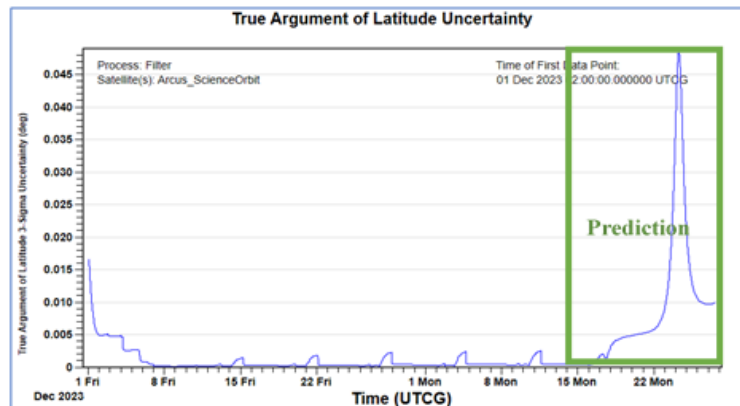


**Figure 17. Filtered 3-σ Uncertainty in True Argument of Latitude, Definitive and Predicted Spans**

We also show this same information modeled in 3-D in STK. The time shown is around the predicted perigee on January 24, 2024. The purple tick-marks along the orbit track are at 30-second intervals, indicating that the 3-sigma uncertainty in the time of perigee is less than 60 seconds. The 3-sigma covariance is shown in light blue, where the in-track direction is largest (around 60 km 3-sigma). The report data on the graphic in yellow displays the 1-sigma covariance displayed near the Jan 24, 2024 perigee. This figure also shows the antenna cone angle from DSS34 during the Jan 24, 2024 perigee. The uncertainty of *Arcus*' predicted position (the predicted covariance shown in light blue) is entirely within the beam-width.

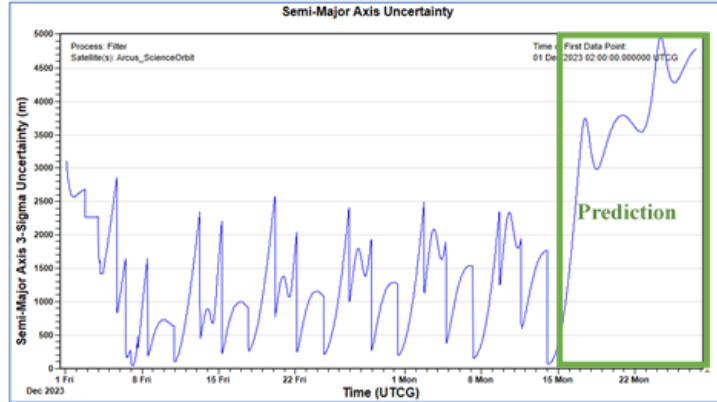


Figure 18. Filtered 3- $\sigma$  Semi-Major Axis Uncertainty, Definitive Span Followed by Predicted Span

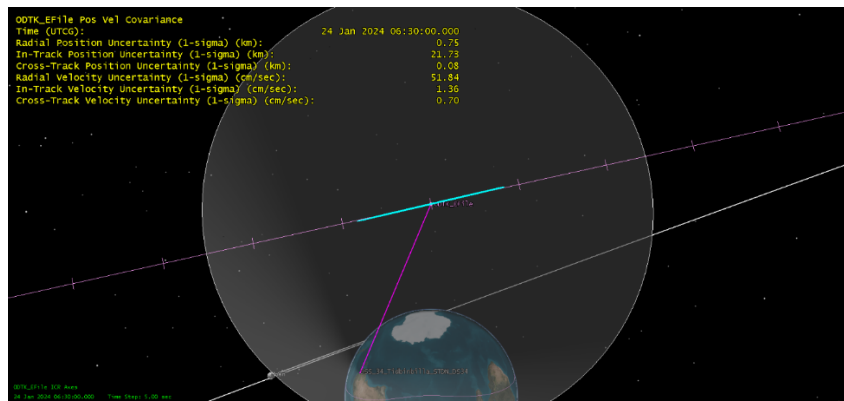


Figure 19: Predicted covariance with DSS34 antenna cone representation

All of these results show that the tracking plan during science operations is sufficient for DSN scheduling and acquisition. More analysis will follow to detail the tracking plan in the early mission phases for maneuver planning and maneuver recovery, as well as describe eclipse prediction uncertainties.

The *Arcus* mission design includes a robust plan to meet and exceed the science mission objectives and is also well-within margins imposed by design drivers. The science orbit design and the orbit determination approach also reflect the desire for simplified long-term mission operations.

## CONCLUSION

P/4 resonance with the Moon is an elegant, practical HEO for science missions such as *Arcus* using intermediate cis-lunar altitudes for data collection and lower altitudes at perigee for downlink. Lunar gravity assist offers affordable perigee raising to clear the Van Allen Belts. The mission orbit requires no maintenance or decommissioning maneuvers, staying clear of GEO indefinitely.

## ACKNOWLEDGEMENTS

The authors would like to recognize Lisa Woloszyn for her extraordinary talent in creating technical images. As always, enduring gratitude goes to the late Professor Harm Buning, whose many students of orbital mechanics included astronauts from Projects Mercury, Gemini, and Apollo.

## REFERENCES

- <sup>1</sup> J. Carrico, D. Dichmann, L. Policastri, et al, “Lunar-Resonant Trajectory Design for The Interstellar Boundary Explorer (IBEX) Extended Mission,” Paper No. AAS 11-454, AAS/AIAA Astrodynamics Specialist Conference, Girdwood, Alaska, USA, August 2011
- <sup>2</sup> J. Carrico et al., “Maneuver Planning and Results for Clementine (The Deep Space Program Science Experiment),” Paper No. AAS 95-129, AAS/AIAA Spaceflight Mechanics Meeting, Albuquerque, New Mexico, USA, February 1995
- <sup>3</sup> M. Loucks, J. Carrico, M. Concha, T. Craychee, “Trajectory Design Operations for the IBEX Mission,” Paper No. AAS 09-134, 19th AAS/AIAA Space Flight Mechanics Meeting, Savannah, Georgia, USA, February 2009
- <sup>4</sup> M. Loucks, L. Plice, D. Cheke, C. Maunder, B. Reich “The LADEE Trajectory as Flown,” Paper No. AAS 15-400, 25th AAS / AIAA Space Flight Mechanics Meeting, Williamsburg, VA, January 11-15, 2015
- <sup>5</sup> J. Parker, M. Lo, “Unstable Resonant Orbits near Earth and Their Applications in Planetary Missions,” in AIAA/AAS Astrodynamics Specialist Conference, Providence, RI, 2004
- <sup>6</sup> M. Mathews, M. Hametz, J.S. Cooley, "High Earth Design for Lunar Assisted Small Explorer Class Missions," in Flight Mechanics/Estimation Theory Symposium, Greenbelt MD, 1994.
- <sup>7</sup> D. McGiffin, M. Mathews, J.S. Cooley, "High Earth Orbit Design for Lunar Assisted Medium Class Explorer Missions," in Flight Mechanics Symposium, Greenbelt MD, 2001.
- <sup>8</sup> J. Gangestad, G. Henningy, R. Persingerz, G. Ricker, “A High Earth, Lunar Resonant Orbit For Lower Cost Space Science Missions,” arXiv:1306.5333v3 [astro-ph.EP] 7 Aug 2013
- <sup>9</sup> D. Dichmann, J. Parker, T. Williams, C. Mendelsohn, “Trajectory Design for the Transiting Exoplanet Survey Satellite” in International Symposium on Spacecraft Flight Dynamics, Laurel MD, May 2014.
- <sup>10</sup> D. Dichmann, R. Lebois, J. Carrico, “Dynamics of Orbits Near 3:1 Resonance in the Earth-Moon System,” The Journal of the Astronautical Sciences (March 2013) ISSN 0021-9142 Volume 60 Number 1, 60:51–86 DOI 10.1007/s40295-014-0009-x, March 2013
- <sup>11</sup> M. Vaquero, K.C. Howell, “Poincaré Maps and Resonant Orbits in the Circular Restricted Three-Body Problem,” Paper No. AAS 11–428, AAS/AIAA Astrodynamics Specialist Conference, Girdwood, Alaska, July 2011.
- <sup>12</sup> J. Carrico, E. Fletcher, “Software Architecture and Use of Satellite Tool Kit’s Astrogator Module for Libration Point Orbit Missions,” Libration Point Orbits and Applications: Proceedings of the Conference, Parador d’Aiguablava, Girona, Spain, June 2002. [Libration Point Orbits and Applications: Proceedings of the Conference Aiguablava, Spain 10 - 14 June 2002; J J Masdemont, Publisher: World Scientific Publishing Company | May 7th, 2003 | ISBN: 9789812383631, ISBN-10 9812383638]
- <sup>13</sup> R. Lebois, L. Policastri, J. Carrico, M. Intelisano, “Extended Mission Maneuver Operations for The Interstellar Boundary Explorer (IBEX),” Paper No. AAS 12-178, 22nd AAS/AIAA Space Flight Mechanics Meeting, Charleston, South Carolina, USA, January 2012
- <sup>14</sup> M. Mesarch, S. Andrews. "The Maneuver Planning Process for the Microwave Anisotropy Probe (MAP) Mission", Paper No. AIAA 2002-4427, AIAA/AAS Astrodynamics Specialist Conference and Exhibit, Monterey, California, 5-8 August 2002
- <sup>15</sup> J. Guzman, D. Dunham, P. Sharer, “STERO Mission Design: Exploiting Matlab, Connect, and Astrogator,” AGI User Exchange, Washington, D.C., 2007
- <sup>16</sup> D. Dunham, J. Mcadams, D. Moessner, D. Ottesen “Contingency plans for MESSENGER’s mercury orbit insertion maneuver,” 10.2514/6.2010-8252, 2010
- <sup>17</sup> Project Jupyter [Computer Software]. (2018). Retrieved from <http://jupyter.org/>
- <sup>18</sup> C. Nickel, J. Carrico, L. Policastri, R. Lebois, R. Sherman, “LADEE Flight Dynamics System Overview,” Paper No. AAS 15-419, 25th AAS / AIAA Space Flight Mechanics Meeting, Williamsburg, VA, January 11-15, 2015
- <sup>19</sup> A. Hawkins, J. Carrico, S. Motiwala, C. MacLachlan, “Flight Dynamics Operations And Collision Avoidance For The Skysat Imaging Constellation,” IWSCFF 17-05, 9th International Workshop on Satellite Constellations and Formation Flying, University of Colorado Boulder, June 19-21, 2017